Egypt. J. Chem. **Vol. 65**, No. 6. pp. 791 - 802 (2022)

Egyptian Journal of Chemistry

http://ejchem.journals.ekb.eg/

Preparation and evaluation of Azo phenol as corrosion inhibitor for carbon steel in acid solution

Mostafa M. Khalefa[c], Hazem F. Khalil[a], S.T.Keera[b], Ashraf M. Ashmawy[a]*

[a] Chemistry Department, Faculty of Science (boys), Al-Azhar University, 11884, (EGYPT).
[b] Egyptian Petroleum Research Institute, Nasr City, 11727, Cairo, Egypt.
[c] chemical lab sector, Petroleum pipeline company, Mostorod, Egypt.
**Corresponding Author: ashraf_ashmawy2002@azhar.edu.eg*

Abstract

In this work, 2,6-di-*tert*-butyl-4-(4-iodophenylazo)phenol (Azo) has been prepared. The chemical structure of this Azo compound has been identified via elemental analysis, Fourier transform infrared spectroscopy (FT-IR), ^{1}Hnuclear magnetic resonance spectroscopy (^{1}H NMR), and mass spectrometry. Furthermore, its ability to inhibit the corrosion of carbon steel in 1 M HCl was studied. Various techniques were used to investigate its inhibition efficiency, including potentiodynamic polarization PDP, electrochemical impedance spectroscopy (EIS), and electrochemical frequency modulation (EFM). It is found that the synthesized compound reveals high inhibition efficiency that is increased as the inhibitor concentration increased. The maximum level of inhibition efficiency has been achieved at an inhibitor concentration of 1×10^{-4} M. The prepared azophenol adsorbed on the steel surface in the form of a mono layer with lateral interlinks between the molecules, according to the adsorption studies. Furthermore, chemisorption is the major adsorption in this situation.

Keywords: Corrosion inhibition, Carbon steel, Azophenol, EDX, PDP

Keywords: Type your keywords here, separated by semicolons ;

1. Introduction

Corrosion in the oilfield produces a variety of problems, including leaks in tanks, casings, tubing, pipelines, and other equipment (1-4), which can complicate operations and maintenance. This frequently results in partial or even entire shutdowns, resulting in significant financial losses exceeding 20% of the maintenance budget (5, 6).Although acids are commonly employed in a variety of industrial applications, including pickling, cleaning, and descaling, they often cause steel equipment to fail, particularly carbon steel. As a result, significant research efforts have been devoted to the study of organic corrosion inhibitors in order to slow down the corrosion process and so avoid economic losses due to metallic corrosion. In acidic media, the majority of well-known organic corrosion inhibitors are aliphatic or aromatic compounds with nitrogen, sulphur, and oxygen atoms in their molecules. Furthermore, the presence of functional groups such as–C=N–,–N=N–, and ROH, as well as aromaticity and electron density at donor atoms, affect corrosion-inhibiting efficacy in hostile solutions (7-11).Inhibitors can be adsorbed on the metal surface either by the formation of coordinate covalent bonds (chemical adsorption) or the electrostatic interaction between the metal and the inhibitor (physical adsorption) (12, 13).The performance of organic inhibitors depends on many factors such as; the presence of electronegative heteroatoms, double bonds, electron-donating or -withdrawing substituent groups, as well as the size of the aromatic ring and the chain length of the hydrocarbon (14-16).

Azo dye derivatives have piqued the interest of scientists due to their numerous applications in a variety of sectors. In 1 M HCl solution, certain benzonitrileazo dyes showed inhibition effectiveness for carbon steel that increased with increasing

DOI: 10.21608/EJCHEM.2022.104441.4933

inhibitor concentration(17). Similarly, azo dyes including 4,5,6,7-tetrahydro-1,3-benzothiazole were tested as anticorrosive agents, and their ability to inhibitthedissolution of mild steel in 1 M HCl solution was established(18). Also in a solution of 1 M HCl, the azo compound; 2,4-dihydroxy-5-((5-mercapto-1H-1,2,4-triazol-3-yl) diazenyl) benzaldehyde was investigated as inhibitor for carbon steel.It has been demonstrated that the inhibition efficiency of that azo compound increases with increasing of its concentration but decreases with rising temperature(19). The effect of iodide ions on the corrosion protection of 3-(4-cyanophenylazo)-2,4-pentanedione for carbon steel in 0.5M H_2SO_4 solution was explored experimentally and theoretically. It has been discovered that the presence of iodide ions improves theinhibition efficiency of that inhibitor(20).The goal of this work was to test phenylazo phenol derivative, such as 2,6-di-tert-butyl-4-(4-iodophenylazo)phenol(AZO), as a novel corrosion inhibitor for carbon steel in 1 M HCl solution using electrochemical methods**.**

2. Experimental

2.1.Materials

All of the reagents used in this research were of analytical grade and didn't require any additional purification(bought from Merk Co., Aldrich, and Fluka Chemical Co.).Carbon steel with the following chemical composition (wt%) has been employed in the corrosion experiments: C, 0.093; P, 0.014; Si, 0.011; Mn, 0.853; Cr, 0.025; Cu, 0.012; Al, 0.032; Ni, 0.013; and Fe, balance. Dilution of laboratory grade 37 % HCl with bi distilled water produced an aggressive solution of 1M HCl.

2.2. Preparation of inhibitors (21)

Azo phenol derivative used in this study wasprepared through two steps:

(i) Diazotization.

4-iodo aniline (0.05mol) was dissolved in 0.05 mol HCl. The mixture was chilled to 0 °C using ice bath. $NaNO_2$ (0.05 mol) was added dropwise while stirring and the temperature was kept at 0°C for 1 hour to get diazonium solution

(ii) Coupling.

0.05 mol 2,6-di-tert-butyl phenol was dissolved in 15 ml aqueous solution of 0.05 mol NaOH, and chilled to 0 °C in using ice bath. The produced diazonium solution was then progressively added to this solution, which was then stirred for 20 minutes. The acidified product was filtered, washed with distilled water, and then recrystallized from acetic acid.

The main scheme of the preparation is shown in Fig.1

2.3. Characterization of the prepared compound

The chemical structure of the prepared compound was ascertained using elemental analysis(elemental analyzer CHNS-932, LECO), infrared (IR) spectroscopy with an (FTIR-type Nicolet iS10 spectrometer), nuclear magnetic resonance (NMR) spectroscopy with tetramethylsilane as an internal standard(Varian 300 MHz spectrometer), and mass spectrometry(SHIMADZU GC/MSQP).

2.4. Electrochemical method

Potentiostat/Galvanostat(Gamry, Reference 3000, Model number 992-00051) was used to perform the electrochemical experiments. A three-electrode cell with a platinum wire ascounter electrode, a saturated calomel electrode as a reference electrode, and carbon steel as a working electrode was used for electrochemical studies. The working electrode was shaped into a cylindrical form of 2 cm length and 1 cm cross-sectional diameter.Only the electrode's cross-sectional area was exposed to the electrolyte after it has been installed in a glass tubing using Araldite. A set of emery papers (grade 320-400-600-800-1000-1200) were used to abrade the electrode surface. After thatit has been washed with distilled water, degreased with acetone, and finally dried in air.After cleaning step, the working electrode has been immersed in 50 ml of 1 M HCl solutionat 298°k, in the absence and presence of various concentrations of the inhibitor(0.50×10^{-6}– 1×10^{-4}M). At a scan rate of 0.5 mV s1, potentiodynamic polarization measurements(PDP)were performed. After immersing the electrode in the aggressive solution for 1 hour and at OCP, EIS was performed. At 298°K, the cell was subjected to a tiny alternating voltage perturbation (10 mV) (peak to peak) spanning a frequency range of 100 kHz to 20 MHz EFM was carried out with a 10 mV AC amplitude and two frequencies of 2 and 5 Hz.

2.6.Surface

After immersion in 1 M HCl solution for 24 hours (in the absence and presence of the inhibitor at the maximum concentration, 1×10^{-4} M),the surface morphology of the tested sample was studied. Scanning electron microscopy (SEM) and energy-dispersive X-ray (EDX) examination were performed on the examined specimen after it has been removed from the solution and dried (JOEL, JSM-T20, Japan).

3. Results and discussion

3.1. Characterization of prepared compound

FTIR, ^{1}HNMR, elemental analysis,and Mass spectra confirmed the structure of 2,6-di-*tert*-butyl-4-(4-iodophenylazo)phenol (Azo), as shown in Figs. 2,3,

and 4, respectively.

- Yield 95%:m.p. 237–239 °C. IR (KBr): ν (cm^{-1}) 3417 (OH),3109–3206 (CHAr), 1604 (–N=N–).^{1}HNMR ppm: for (DMSO) δ=2.502, δ=7.8 (s, 1H, -OH) , δ=6.93 (d, 4H, aromatic H for iodo),δ=7.19 (s, 2H, aromatic H), δ=1.075 (s, 1H, -CCH_3), δ=1.246 (s,1H, -CCH_3),δ=1.344(s, 1H, -CCH_3) ,δ=1.388 (s, 1H, CCH_3), δ=1.437 (s,1H, -CCH_3),Anal. Calc. for C 55.05, H 5.78, N6.42% found: C 55.21, H 5.83, N 6.64%. MS: m/z 436.33, m/z found: 436.02

3.2. Electrochemicalmeasurements

3.2.1. Potentiodynamic polarization technique

Figure 5 show the PDP curves for carbon steel in 1 M HClin the absence and presence of the synthesized compound at concentrations of (0.50×10^{-6}–1×10^{-4}M) at298°k.Table 1 presentsthe values of electrochemical parameters like corrosion current density (I_{corr}), corrosion potential (E_{corr}), cathodic and anodic Tafel slopes (βc and βa), and inhibition efficiency. The findings clearly show that the synthesizedinhibitor reduces the corrosion rate by shifting both the anodic and cathodic branches of the Tafel plots to lower current density values at all concentrations.Table 1 shows that the values of (βc)changed due to a change in inhibitor concentration, which reduced hydrogen evolution by cathodicreduction, the values of (βa) changed due to adsorption of inhibitor molecules on the surface of carbon steel by anodic reaction, and the values of (I_{corr}) decreased due to adsorption of inhibitor molecules on the surface of themetal and blocking the active sites by cathodic and anodic reactions. We can see from the table and figures that increasing the inhibitor concentration decreases the corrosion rate.

The inhibition efficiency (IE %) and thedegree of surface coverage (Θ) were calculated using the following equations(22):

$$\Theta = [(I_{0corr} - I_{corr})/I_{0corr}] \quad (1)$$

$$IE\% = [(I_{0corr} - I_{corr})/I_{0corr}]\times 100 \quad (2)$$

WhereI_{corr} and I_{0corr} denote the inhibited and uninhibited corrosion current densities, respectively**.**

3.2.2. EIS measurements

Table 2.Electrochemical impedance spectroscopy parameters; slopes of the Bode impedance magnitude at intermediate frequencies (S), and maximum phase angle values (α°) for the corrosion of steel in 1 M HCl in the absence and presence of different concentrations of the prepared compound at 298°k

After immersing the electrode in 1 M HCl for 1 hour in the presence and absence of various inhibitor concentrations ranging from ($0.05\ x10^{-5}$ – $10\ x10^{-5}$M),EIS was recorded at open-circuit potential (OCP) with a tiny alternating voltage perturbation (10 mV) imposed on the cell spanning a frequency range of 100 kHz to 20 MHz at 298°K and is displayed as Nyquist plots and Bode plots in Fig.6.

The Nyquist plots in 1 M HCl at OCP and 298°k with and without the Azocompound are shown in Fig. 6, and the results are listed in Table 2. This reaction follows the Faraday process, which ensures that a single charge transfer resistance is present in parallel with the double-layer capacitance element [16].This indicated that charge transfer occurs at the electrode/solution interface, that the mode of transfer determines corrosion reaction, and that the presence of inhibitors has no effect on the steel dissolution mechanism[17].

The figure shows a consistent shape across all tested concentrations, demonstrating that the corrosion mechanism did not alter as a result of the addition of this inhibitor (23).

However, the diameter of this semicircle increasesin the presence of inhibitor than in the absence of inhibitor, and it also increases with increasing inhibitor concentrations, showing that the inhibitor reveals significant corrosion resistance.The analogous circuit consists of a double-layer capacitance (Cdl) in parallel with a charge transfer resistance (Rct), which was previously used to represent the iron/acid interface, and a similar circuit for acidic corrosion inhibition of steel has been described in the literature [16, 17].

The variation in solution resistance (Rs), charge transfer resistance (Rct), and double-layer capacitance (Cdl) is summarized in table 2. As can be seen, the values of Rs are quite low when compared to the values of Rct. The value of Rct increases as the inhibitor concentrations increase, whereas the value of double-layer capacitance (Cdl) decreases. Cdl decrease when the local dielectric constant decrease and/or the thickness of the electrical double layer increases, indicating that the inhibitoradsorbed at the metal/solution interface (24).The following equation (25):was used to compute the inhibitory efficiency:

$$\Theta = [(R_{oct} - R_{ct})/R_{oct}] \quad (3)$$

$$\eta_z\% = [(R_{oct} - R_{ct})/R_{oct}] \times 100 \quad (4)$$

Where Rct and $R_o$ctdenotethe charge transfer resistances with and without the inhibitor, respectively.The inhibition efficiency increases with the increase ofconcentration of the inhibitor.

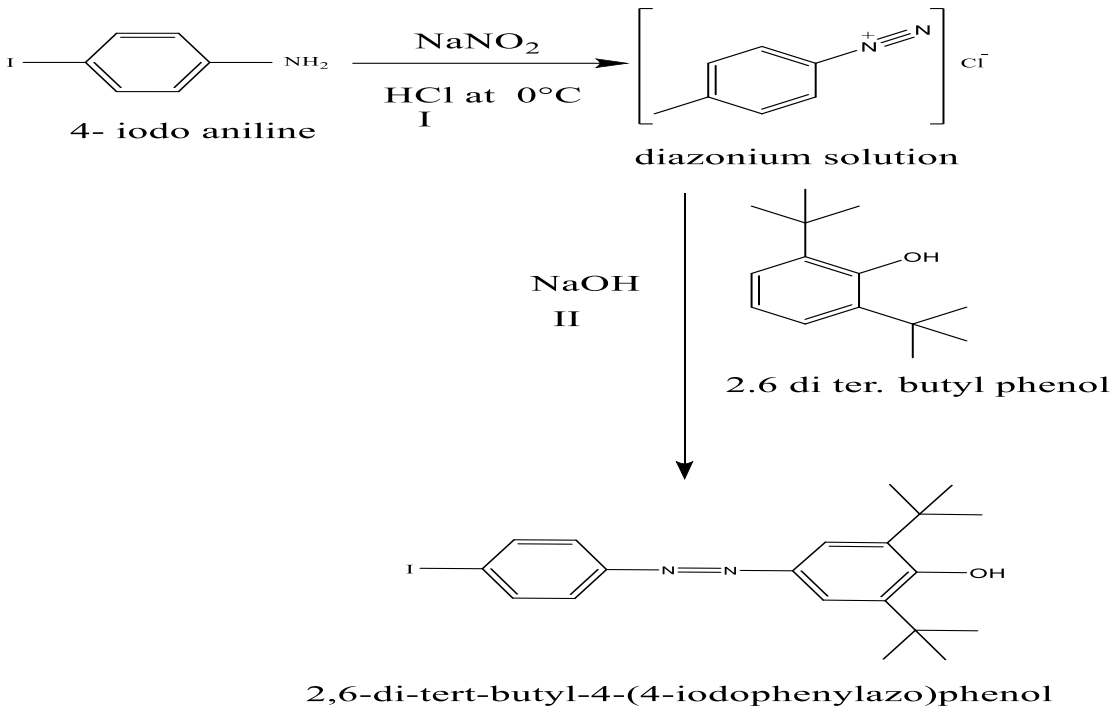

Fig.1. Schematic diagram for preparation of 2,6-di-*tert*-butyl-4-(4-iodophenylazo)phenol.

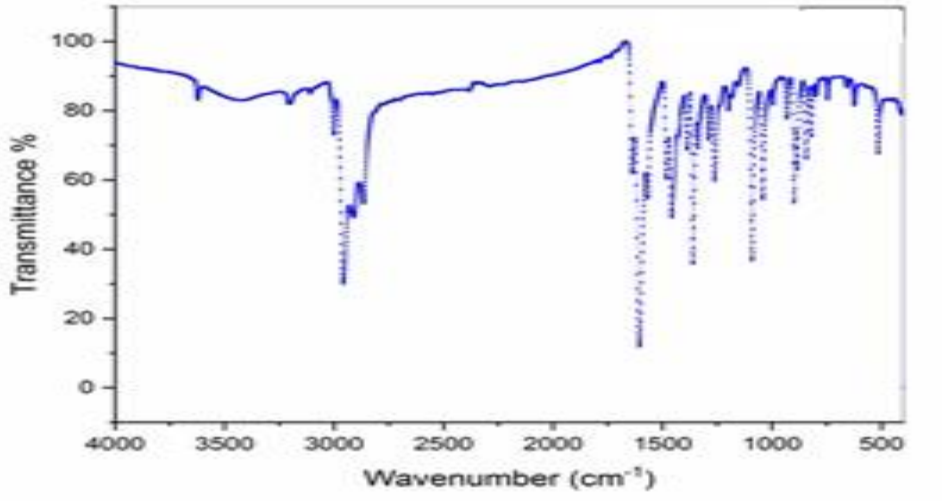

Fig.2. The FTIR spectra for 2,6 Di-tert.-butyl -4-(4-iodo-phenylazo)- phenol.

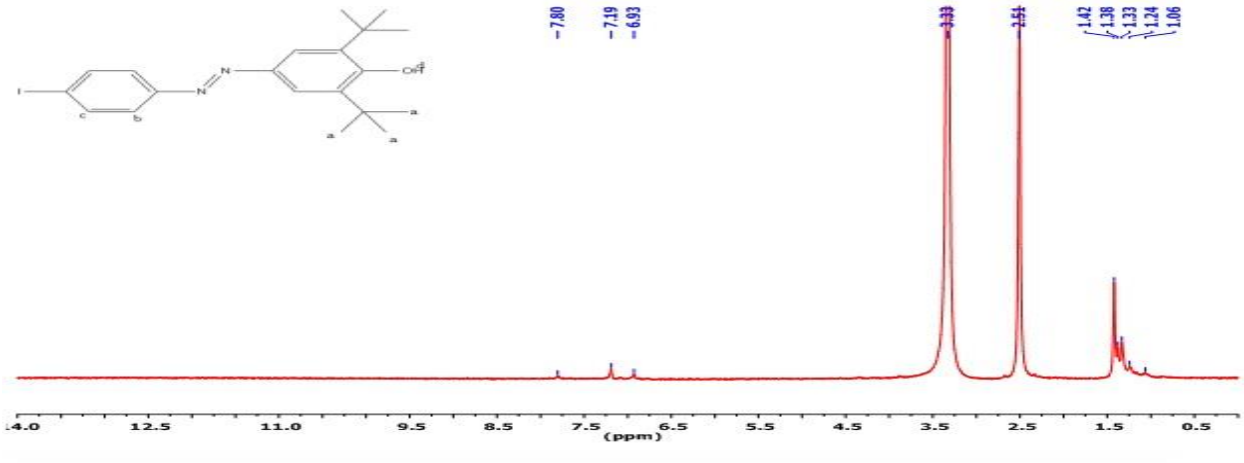

Fig.3. [1]HNMR spectra of 2,6 Di-tert.-butyl -4-(4-iodo-phenylazo)- phenol.

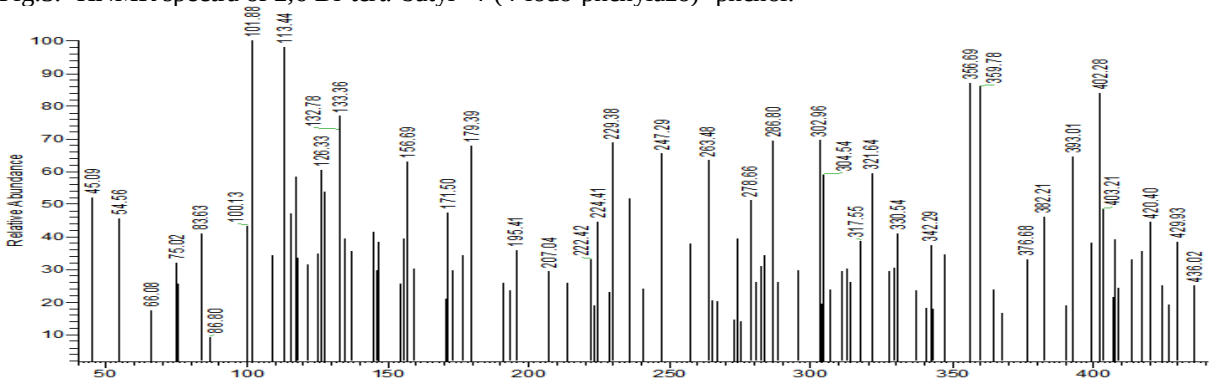

Fig.4.Mass spectrumof 2,6 Di-tert.-butyl -4-(4-iodo-phenylazo)- phenol.

.

Table 1.Corrosion parameters calculated form potentiodynamic polarization measurements in 1M HCl in the absence and presence of various concentrations of the synthesized compound at 298°K

Cpd.	**Conc. (M) $X10^{-5}$**	**I corr. (µA cm^{-2})**	**Ecorr. (mVvsSCE)**	**ßa (mV dec^{-1}) X 10^{-3}**	**ßc (mV dec^{-1}) X 10^{-3}**	**K (mpy)**	**Ɵ**	**IE %**
Blank	0.00	606	−340	84.00	95.40	276.7	----	----
Azo	0.05	255	−435	163.8	111.9	116.4	0.5793	57.93
	0.50	246	−350	69.40	107.2	112.6	0.5931	59.31
	1.00	206	−436	150.9	131.6	94.24	0.6594	65.94
	5.00	193	−403	108.0	125.3	88.00	0.6820	68.20
	10.0	172	−408	112.8	120.0	78.44	0.7165	71.65

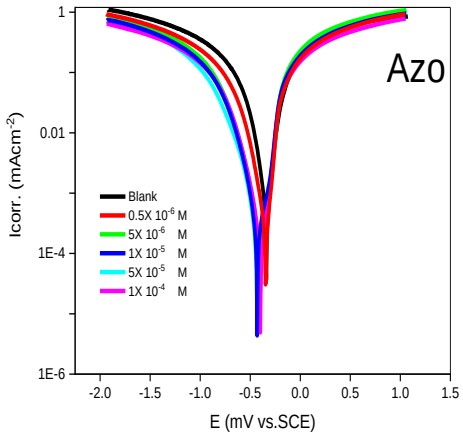

Fig.5.Potentiodynamic polarization curves of the synthesizedcompound in the presence and absence of various inhibitor concentrations at 298°k.

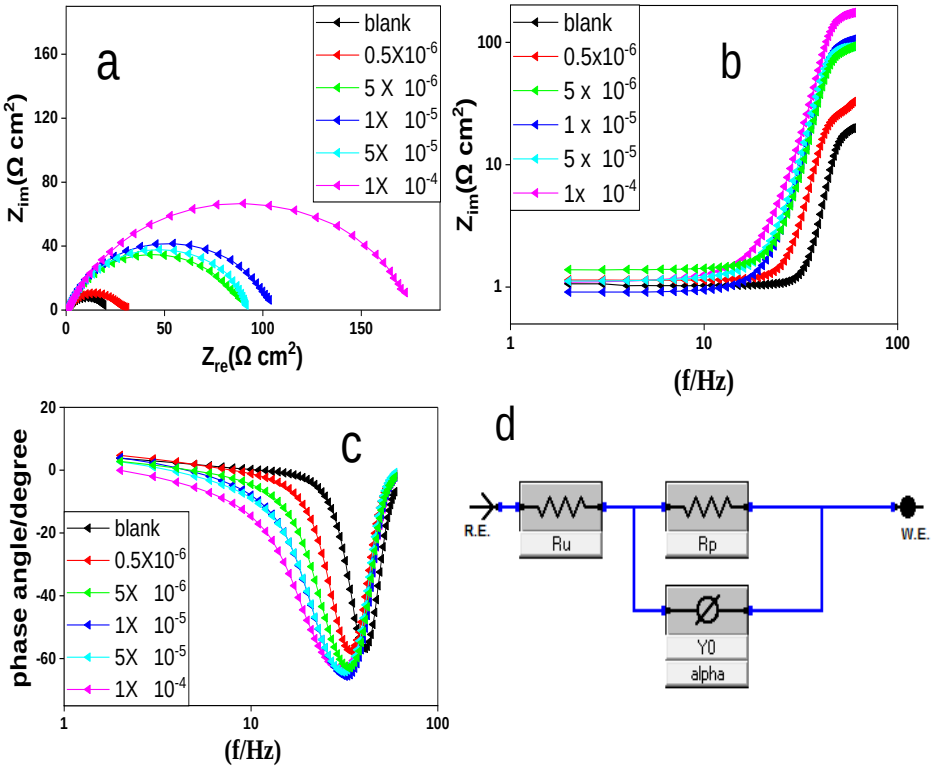

Fig.6.Nyquist(a), Bod (b) and phase angle plots(c) of EISfor the corrosion of steel in 1M HCl in the absence and presence of different concentrations of Azo compound at 298 °k..

Table 2.Electrochemical impedance spectroscopy parameters; slopes of the Bode impedance magnitude at intermediate frequencies (S), and maximum phase angle values (α°) for the corrosion of steel in 1 M HCl in the absence and presence of different concentrations of the prepared compound at 298°k

Cpd.	Conc. (M) $X10^{-5}$	$R_s(R_u)$ (Ω cm^2)	$R_{ct}(R_p)$ (Ω cm^2)	Y_o (μ $\Omega^1 s^n cm^2$) X 10^{-3}	N	C_{dl} ($\mu F cm^{-2}$)	Chi-squared $X10^{-3}$	Θ	η_z %
Blank	0.00	1.038	18.88	4.478	0.899	3391.65	0.353	-----	----
	0.05	1.401	88.70	0.445	0.856	264.92	0.489	0.7871	78.71
	0.50	1.149	92.93	0.325	0.850	175.92	0.583	0.7968	79.68
	1.00	0.913	104.6	0.419	0.848	239.51	0.601	0.8195	81.95
	5.00	0.849	162.0	0.206	0.860	118.44	0.302	0.884	88.40
	10.0	1.109	178.2	0.298	0.803	145.36	0.418	0.8940	89.40

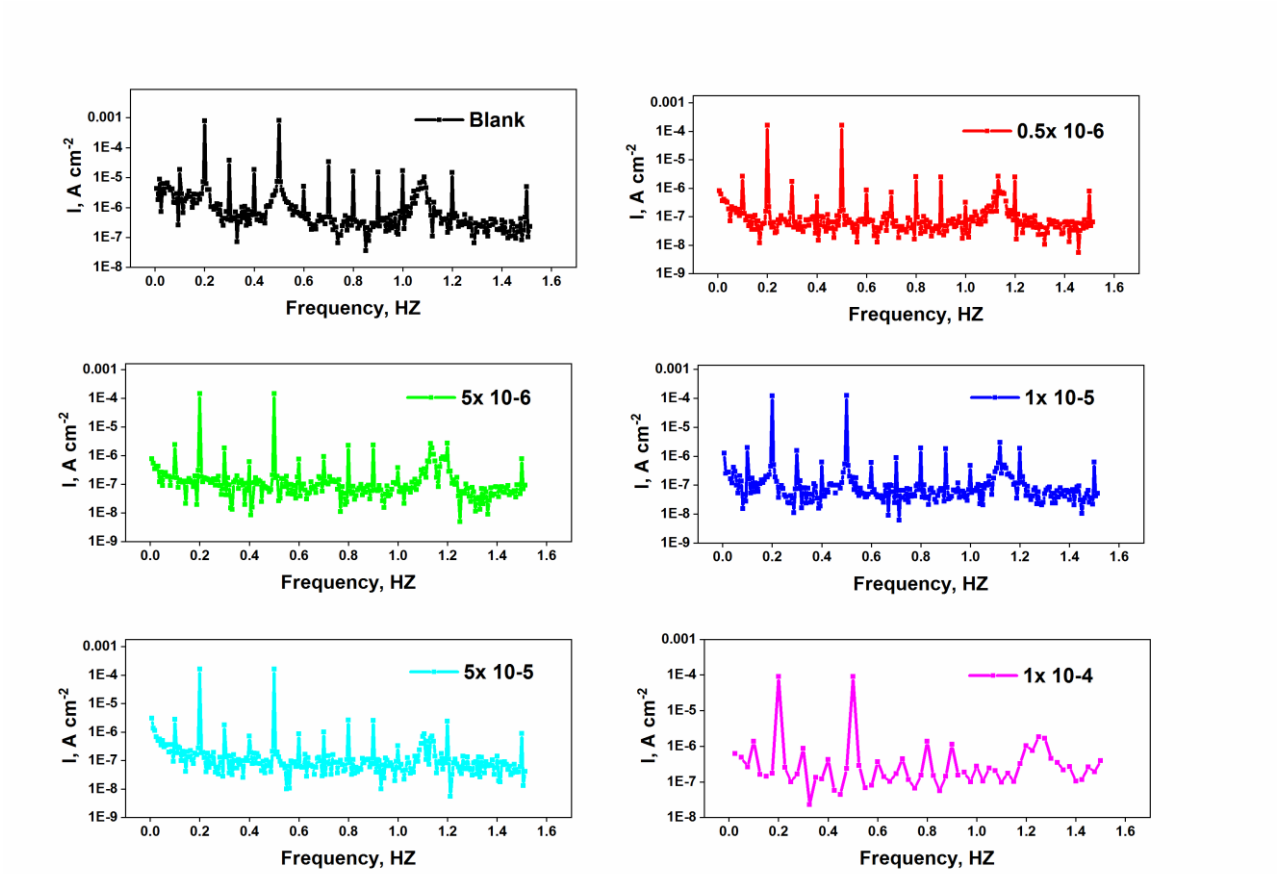

Fig.7.EFM spectra for corrosion of carbon-steel in 1 M HCl in the absence and presence of different concentrations of inhibitor Azo at 298ºk

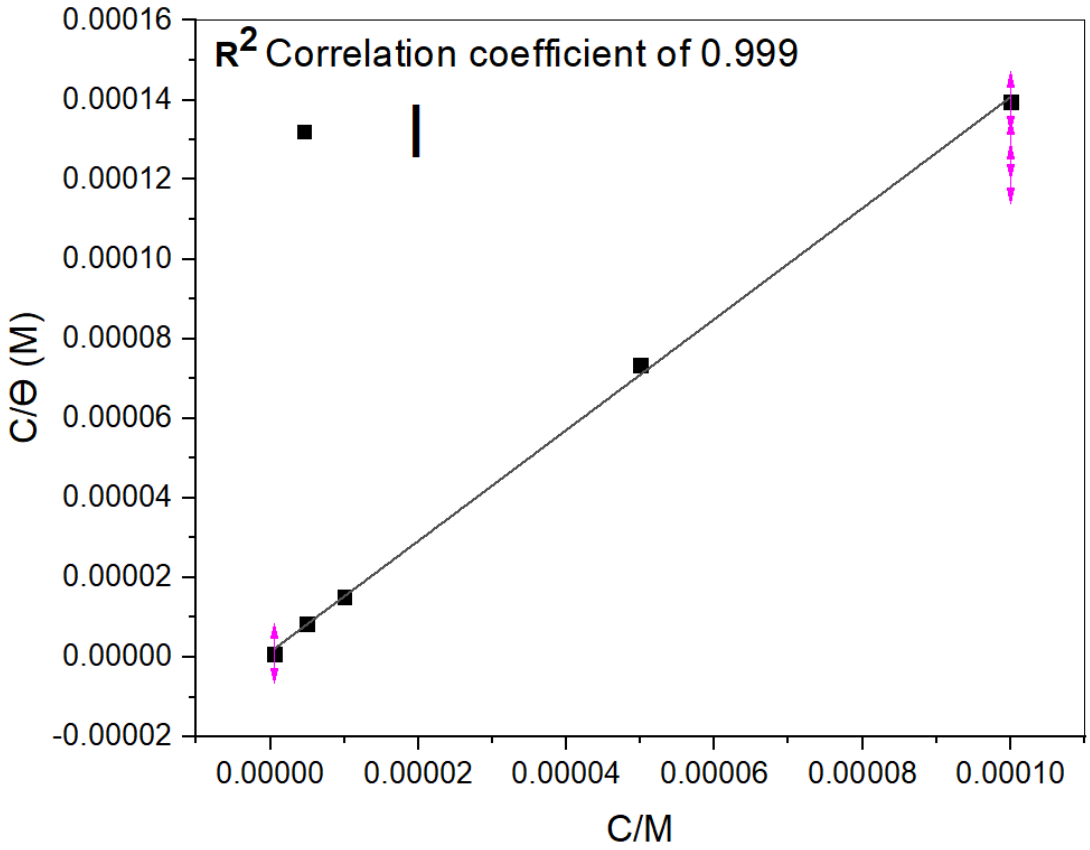

Fig.8. Langmuir isotherm [C/θ] vs. [C] of inhibitor(Azo)for corrosion of steel in 1 MHCl at 298ºK

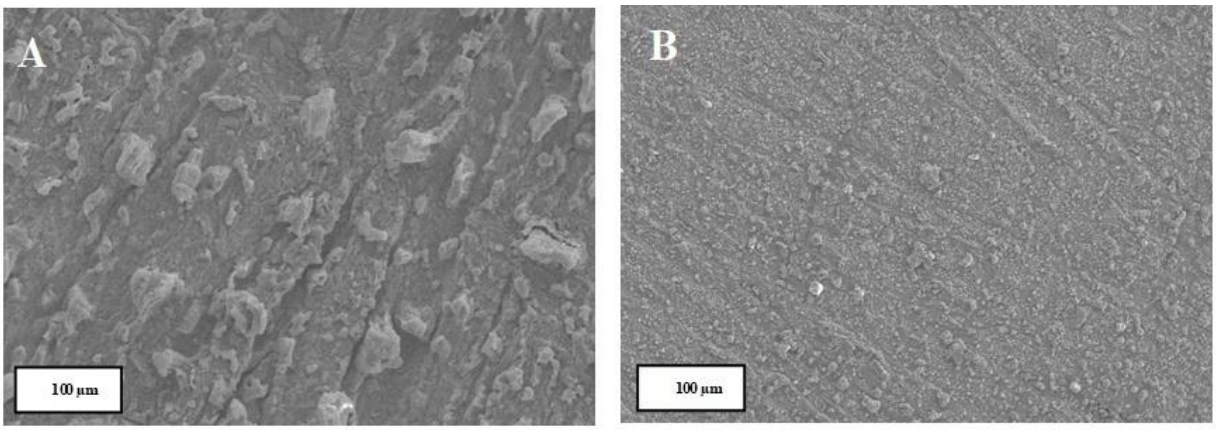

Fig.9.Scanning electron micrographs of the tested samples,(A) blank, B sample with (1×10^{-4}M) of Azoinhibitor.

Table 3. Electrochemical kinetic parameters obtained via electrochemical frequency modulation for the corrosion of steel in the absence and presence of various concentrations of the prepared Azocompound in 1 M HCl at 298°k.

Cpd.	Conc. (M) X 10^{-5}	Icorr. (µA cm^{-2})	βa (mV dec^{-1}) x10^{-3}	Bc (mV dec^{-1}) x10^{-3}	CF-2	CF-3	k (mpy)	Θ	η_{EFM} %
Blank	**0.00**	**1.007**	**73.76**	**92.82**	**2.033**	**3.191**	**460.3**	___	___
Azo	0.05	231.4	90.39	94.36	3.026	3.076	105.7	0.7704	77.04
	0.50	202.8	87.22	91.87	2.792	3.145	92.68	0.7986	79.86
	1.00	174.6	90.21	95.60	2.273	3.070	79.78	0.8267	82.67
	5.00	230.8	89.18	93.54	2.633	2.974	105.5	0.7708	77.08
	10.0	136.3	96.38	100.7	1.875	3.244	62.27	0.8647	86.47

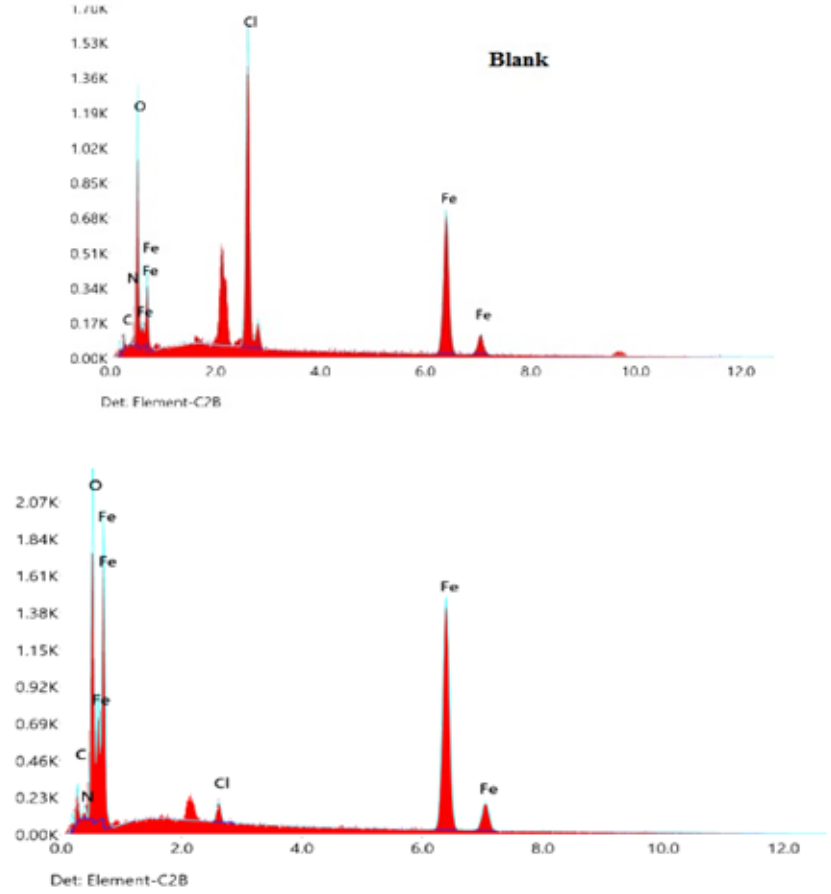

Fig.10. The EDX patterns of the film formed on carbon steel surface after immersion in HCl in absence and presence of the investigated inhibitor.

Table 4.Weight percentages of elements on the steel surface in the presence and absence of 1 × 10^{-4} M ofAzoinhibitor by energy-dispersive X-ray analysis

Specimen	Fe wt%	O wt%	Cl wt%	C wt%	N wt%
Mild steel in (1 M HCl)	47.6	28.6	17	0.09	---
Mild steel in (1 M HCl + Azo)	70.2	13.2	1.3	12.6	2.7

3.2.3. EFM of carbon steel in 1 M HCl

EFM has recently emerged as a new corrosion measurement technique that doesn't require prior knowledge of the Tafel constants (26).The current responses occur at higher frequencies than the applied signal, such as zero harmonic and intermodulation frequencies, when one or more sine waves are used to aid a potential disturbance. Corrosion rate, Tafel parameters, and causality factors (CF-2 and CF-3) are all measured in a single dataset with this method. To get a current response in the EFM, every corroding specimen is subjected to a potential perturbation signal composed of two sine waves.It may also be used to precisely measure corrosion parameters for various metals and electrolytes combinations. CF-2 and CF-3 have standard values of 2.0 and 3.0, respectively, suggesting legitimate EFM data. Different values indicate that noise has impacted the measurement.

Figure 7 shows the EFM spectra for carbon steel corrosion in 1 M HCl at 298°K, which includes current responses assigned to harmonic and intermodulation current peaks.I_{corr}, Tafel slopes βc and βa, and CF-2 and CF-3 were calculated from the larger peaks, and the results are provided in Table7. It has been established that as the inhibitor concentration increased, the corrosion current densities of carbon steel decrease.

The largest peak were used to calculate all kinetic factors derived from EFM, such as I_{corr},βc, βa, and CF-2 and CF-3, which were then gathered in Table 3. The ηEFM % and ɵ were calculated using the following equation[22]

$$\eta EFM = \Theta \times 100 = (I_{0corr} - I_{corr})/ I_{0corr} \times 100 \quad (5)$$

As I_{0corr}andI_{corr}representing the current densities for the corrosion solutions that does not contain and contain the inhibitors, respectively.

3.2.4. Mechanism of corrosion

The adsorption isotherm can be used to describe the types, sites, and frequency of mutual interactions between a metal surface and an inhibitor. When a metal is put to a corrosive medium, it has a relationship between its surface coverage and the inhibitor concentration (C). The Langmuir adsorption isotherm, as shown in thefollowing equation, better explains the azo compound adsorption on mild steel surfaces(27).The data fromPDP was used to solve the following equation:

$$\frac{c}{\theta} = \frac{1}{\text{kads}} + c \quad (6)$$

Where: $K_{ads}$is the equilibrium constant of the inhibitor adsorption process and C is the inhibitor concentration.From figure 8, K_{ads}value is$7.4x10^5$.The higher values of K_{ads} indicate stronger adsorption of Azo in the surface of carbon steel(28, 29).The free energy values of adsorption (ΔG^0_{ads})were calculated using thefollowing equation (30):

$$\Delta G^0_{ads} = - RT \ln(55.5\ K_{ads}) \quad (7)$$

where the factor 55.5 represents the concentration of watermolecules in the solution (in mole/l) and R is the universal gas constant (8.314 J K^{-1} mol^{-1}). ΔG^0_{ads} value of -43.43KJmol^{-1}, confirming the spontaneous adsorption of Azo molecule. The dominant adsorption for this case ischemisorptions(31, 32).

3.3.Morphology

3.3.1. Scanning Electron Microscope (SEM) analysis

SEM micrographs of the examined specimens in the absence and presence of the inhibitor at the highest concentration of 1× 10^{-4} M are shown in Figure 9. In the absence of the inhibitor, the surface of the steel specimen corroded in 1 M HCl revealing deep black grooves with grey zones, which match to the dandruff of the generated corrosion products. Meanwhile, in the presence of theAzoinhibitor, which was uniformly distributed across the steel specimen's surface, no grooves were observed. As validated by SEM analysis, the adsorbed inhibitor appeared as

white spots covering the whole surface of the tested steel specimen(33).

3.3.2.Energy Dispersive X-ray(EDX) analysis

To confirm the adsorption of the inhibitor on the surface of steel specimens, EDX was used to quantify the components present and their percentages (Table 4). The presence of oxygen and iron with a weight percentage equal to their percentage in iron hydroxide, as well as a high weight percentage of chloride ions, was confirmed by EDX analysis for the steel sample evaluated in the absence of the inhibitor. On the other hand, the steel specimen evaluated in the presence of the inhibitorhad a high carbon and nitrogen content. The adsorption of the inhibitor on the steel surface is the sole explanation for this result.Furthermore, there was a significant decrease in the weight proportion of oxygen and chloride ions. The EDX patterns of the film generated on a carbn steel surface in the absence and presence of the investigated inhibitor are shown in Figure 10.

Conclusion

Based on the experimental results, the following main conclusions can be considered:

1. Azo phenol derivative prepared and characterized by IR,^{1}HMR and mass spectroscopy.

2. This compound was evaluated by different electrochemical techniques as effective corrosion inhibitors for carbon steel in 1 M HCl.
3. In the presence of the prepared inhibitor, SEM and EDX investigations demonstrated the formation of a protective film on the metal surface.
4. Inhibition efficiency of prepared azo phenol increases with the increasing of the concentration of the inhibitor.
5. This inhibitor can be used effectively in many industries where HCl is involved to protect carbon steel from corrosion

References

[1] .Botirovna GR, Jumagulovich MK, Uralovna XZ: studies of the anticorrosive properties of sulfur-containing bicyclic α-aminoketones. *Journal of Critical Reviews* 2020, 7:283-286.

[2] .El-Meleigy AE, Youssef G, El-Shayeb HA, El-Shamy AM: Corrosion and corrosion protection of aluminum in hydrochloric acid by using piperidine. *Ochrona przed Korozją* 2014:66--71.

[3] .Abou-Elseoud WS, Abdel-karim AM, Hassan EA, Hassan ML: Enzyme-and acid-extracted sugar beet pectin as green corrosion inhibitors for mild steel in hydrochloric acid solution. *Carbohydrate Polymer Technologies and Applications* 2021, 2:100072.

[4] Mandour HS, Abdel-Karim AM, Fathi AM: Inhibition Efficiency of Copper Corrosion in a Neutral Chloride Solution by Barbituric and Thiobarbituric Acids. Portugaliae Electrochimica Acta2021, 39: 85-103.

[5] Garcia-Arriaga V, Alvarez-Ramirez J, Amaya M, Sosa E: H_2S and O_2 influence on the corrosion of carbon steel immersed in a solution containing 3 M diethanolamine. *Corrosion Science* 2010, 52:2268-2279.

[6] Sherif E-SM, Abbas AT, Gopi D, El-Shamy A: Corrosion and corrosion inhibition of high strength low alloy steel in 2.0 M sulfuric acid solutions by 3-amino-1, 2, 3-triazole as a corrosion inhibitor. *Journal of Chemistry* 2014, 2014.

[7] Fouda A, Ellithy A: Inhibition effect of 4-phenylthiazole derivatives on corrosion of 304L stainless steel in HCl solution. *Corrosion Science* 2009, 51:868-875.

[8] Hamani H, Douadi T, Al-Noaimi M, Issaadi S, Daoud D, Chafaa S: Electrochemical and quantum chemical studies of some azomethine compounds as corrosion inhibitors for mild steel in 1 M hydrochloric acid. *Corrosion science* 2014, 88:234-245.

[9] Shokry H: Molecular dynamics simulation and quantum chemical calculations for the adsorption of some Azo-azomethine derivatives on mild steel. *Journal of Molecular Structure* 2014, 1060:80-87.

[10].Zhang F, Tang Y, Cao Z, Jing W, Wu Z, Chen Y: Performance and theoretical study on corrosion inhibition of 2-(4-pyridyl)-benzimidazole for mild steel in hydrochloric acid. *Corrosion Science* 2012, 61:1-9.

[11].El-Shamy A, Shehata M, Gaballah ST, Elhefny EA: Synthesis and evaluation of ethyl (4-(n-(thiazol-2-yl) sulfamoyl) phenyl) carbamate (tspc) as a corrosion inhibitor for mild steel in 0.1 M HCl. *Adv Chem* 2015, 11.

[12] Al-Noaimi MZ, Saadeh H, Haddad SF, El-Barghouthi MI, El-Khateeb M, Crutchley RJ: Syntheses, crystallography and spectroelectrochemical studies of ruthenium azomethine complexes. *Polyhedron* 2007, 26:3675-3685.

[13] Masoud M, Awad M, Shaker M, El-Tahawy M: The role of structural chemistry in the inhibitive performance of some aminopyrimidines on the corrosion of steel. *Corrosion Science* 2010, 52:2387-2396.

[14].Verma C, Ebenso EE, Quraishi M: Molecular structural aspects of organic corrosion inhibitors: influence of–CN and–NO_2 substituents on designing of potential corrosion: inhibitors for aqueous media. *Journal of Molecular Liquids* 2020:113874.

[15].Sherif E-SM, Abbas AT, Halfa H, El-Shamy A: Corrosion of high strength steel in concentrated sulfuric acid pickling solutions and its inhibition by 3-amino-5-mercapto-1, 2, 3-triazole. *Int J Electrochem Sci* 2015, 10:1777-1791.

[16].Shahen S, Gaber G: 4-Aminobenzenesulfonic acid as Effective Corrosion Inhibitor for carbon steel in hydrochloric acid. *Egyptian Journal of Chemistry* 2021, 64:825-834.

[17].Fouda A, El-Azaly AH, Awad R, Ahmed A: New benzonitrile azo dyes as corrosion inhibitors for carbon

steel in hydrochloric acid solutions. *Int J Electrochem Sci* 2014, 9:1117-1131.
[18] Mallikarjuna N, Keshavayya J, Prasanna B, Praveen B, Tandon H: Synthesis, characterization, and anti-corrosion behavior of novel mono azo dyes derived from 4, 5, 6, 7-Tetrahydro-1, 3-benzothiazole for mild steel in acid solution. *Journal of Bio-and Tribo-Corrosion* 2020, 6:1-17.
[19] Fouda A, El-morsi M, Gaber M, Fakeeh M: Azo Compounds as Green Corrosion Inhibitor for Carbon Steel in Hydrochloric Acid Solution: Corrosion Inhibition and Thermodynamic Parameters. *Int J Electrochem Sci* 2017, 12:8745-8760.
[20] Boucherit L, Al-Noaimi M, Daoud D, Douadi T, Chafai N, Chafaa S: Synthesis, characterization and the inhibition activity of 3-(4-cyanophenylazo)-2, 4-pentanedione (L) on the corrosion of carbon steel, synergistic effect with other halide ions in 0.5 M H2SO4. *Journal of molecular structure* 2019, 1177:371-380.
[21] Ashmawy AM, Attia SK, Nessim MI, Elnaggar EsM, El-Bassoussi AA: Study on some azo liquid crystals as antioxidants for local base oil. *Molecular Crystals and Liquid Crystals* 2018, 668:78-90.
[22] Deyab M, Keera S: Effect of nano-TiO2 particles size on the corrosion resistance of alkyd coating. *Materials Chemistry and Physics* 2014, 146:406-411.
[23] Labjar N, Lebrini M, Bentiss F, Chihib N-E, El Hajjaji S, Jama C: Corrosion inhibition of carbon steel and antibacterial properties of aminotris-(methylenephosphonic) acid. *Materials Chemistry and Physics* 2010, 119:330-336.
[24] Khaled K, Hackerman N: Investigation of the inhibitive effect of ortho-substituted anilines on corrosion of iron in 1 M HCl solutions. *Electrochimica Acta* 2003, 48:2715-2723.
[25] Deyab M, Abd El-Rehim S, Keera S: Study of the effect of association between anionic surfactant and neutral copolymer on the corrosion behaviour of carbon steel in cyclohexane propionic acid. *Colloids and Surfaces A: Physicochemical and Engineering Aspects* 2009, 348:170-176.
[26] Hermas A, Morad M: A comparative study on the corrosion behaviour of 304 austenitic stainless steel in sulfamic and sulfuric acid solutions. *Corrosion Science* 2008, 50:2710-2717.
[27] Singh AK, Ebenso EE: Effect of Ceftezole on the corrosion of mild steel in HCl solution. *Int J Electrochem Sci* 2012, 7:2349-2360.
[28] Jeeva M, susai Boobalan M, Prabhu GV: Adsorption and anticorrosion behavior of 1-((pyridin-2-ylamino)(pyridin-4-yl) methyl) pyrrolidine-2, 5-dione on mild steel surface in hydrochloric acid solution. *Research on Chemical Intermediates* 2018, 44:425-454.
[29] Kumar CBP, Mohana KN, Muralidhara HB: Electrochemical and thermodynamic studies to evaluate the inhibition effect of synthesized piperidine derivatives on the corrosion of mild steel in acidic medium. *Ionics* 2015, 21:263-281.
[30] Quartarone G, Battilana M, Bonaldo L, Tortato T: Investigation of the inhibition effect of indole-3-carboxylic acid on the copper corrosion in 0.5 M H_2SO_4. *Corrosion Science* 2008, 50:3467-3474.
[31] Hegazy M, El-Tabei A, Bedair A, Sadeq M: An investigation of three novel nonionic surfactants as corrosion inhibitor for carbon steel in 0.5 M H_2SO_4. *Corrosion Science* 2012, 54:219-230.
[32] Yadav DK, Quraishi M, Maiti B: Inhibition effect of some benzylidenes on mild steel in 1 M HCl: an experimental and theoretical correlation. *Corrosion science* 2012, 55:254-266.
[33] Ashmawy AM, Mostfa M: Study of Eco-Friendly Corrosion Inhibition for Mild Steel in Acidic Environment. *Egyptian Journal of Chemistry* 2021, 64:1285-1291.